

Neotectonic setting of the North American plate in relation to the Chicxulub impact.

Gregory C Herman, New Jersey Geological Survey
PO Box 427, Trenton, NJ 08625
greg.herman@dep.state.nj.us

The neotectonic setting of the North American plate (NAP) is mapped using terrestrial geophysical data with geographic information systems. NASA's GPS records of crustal plate motion show rotation of the NAP and the Caribbean plate about a hub that is circumferential to the Chicxulub impact crater (~65 Ma). Outboard rings of crustal uplift and subsidence occur at punctuated intervals from the hub center where plate convergence involves multiple subduction zones in the Central American region. The vertical component of current plate motion on Earth is delineated utilizing a triangulated integrated network surface. Currently rising and subsiding areas in the NAP continental interior reflect the multi-ring basin architecture, as do regional Bouger gravity anomalies in the west-central Atlantic. A scatter plot of the horizontal component of plate motion for the NAP vs. distance from impact shows an abrupt increase in plate motion at 2900-km, the same distance from impact as the depth to the core-mantle boundary. The impact produced multi-ring percussion structures in the NAP with crustal arches centered about 1600 and 2900 km from impact, both distances corresponding to active intraplate seismogenic zones, and the latter distance corresponding with the Laramide and Adirondack epeirogenic uplifts. NAP sub-plate boundaries may involve zones of crustal fracturing and faulting lying above mantle-rooted structures having the geometry of spherical percussion shells. A geometric model of crustal rotation and associated fractures preceding and following the impact is consistent with overlapping fracture systems mapped in the Triassic-Jurassic Newark basin. The model depicts a switch in NAP rotation polarity and regional stress from clockwise extension preceding impact to counterclockwise compression postdating it. The NAP plate rotation pole also flips from high northern latitudes before impact to an equatorial position afterwards. If this hypothesis is confirmed, impact tectonics is certain to play an important role in plate tectonic theory by elucidating large epeirogenic crustal episodes, as well as effecting wholesale changes in regional plate dynamics.

What do we know about the Chicxulub impact?

- Originally proposed by Luis and Walter Alvarez (1979-80) based on Iridium anomalies found in an ash layer in Italy, and subsequently throughout the world.

- Occurred at around 65 mya, possibly in conjunction with a multiple-impact episodes over hundreds of thousands years that essentially brought the Cretaceous period of the dinosaurs to an end.

- These findings led to an extensive search for a large impact crater that is 65 million years old. Seven researchers finally located the impact site on Mexico's Yucatan Peninsula (early 1990's).

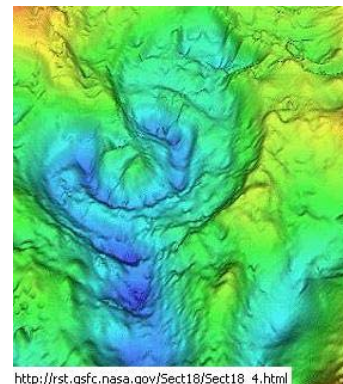
- It is a huge buried impact crater that is called Chicxulub, a Maya word that roughly translates as "tail of the devil." The crater is approximately 150-300 km wide, lies buried beneath a kilometer-thick sequence of sediments, and has been imaged using geophysical techniques.

- The asteroid or comet that produced the Chicxulub crater was about 10-20 km in diameter. When an object that size hits Earth's surface, it causes a tremendous shock wave while transferring energy and momentum to the ground.

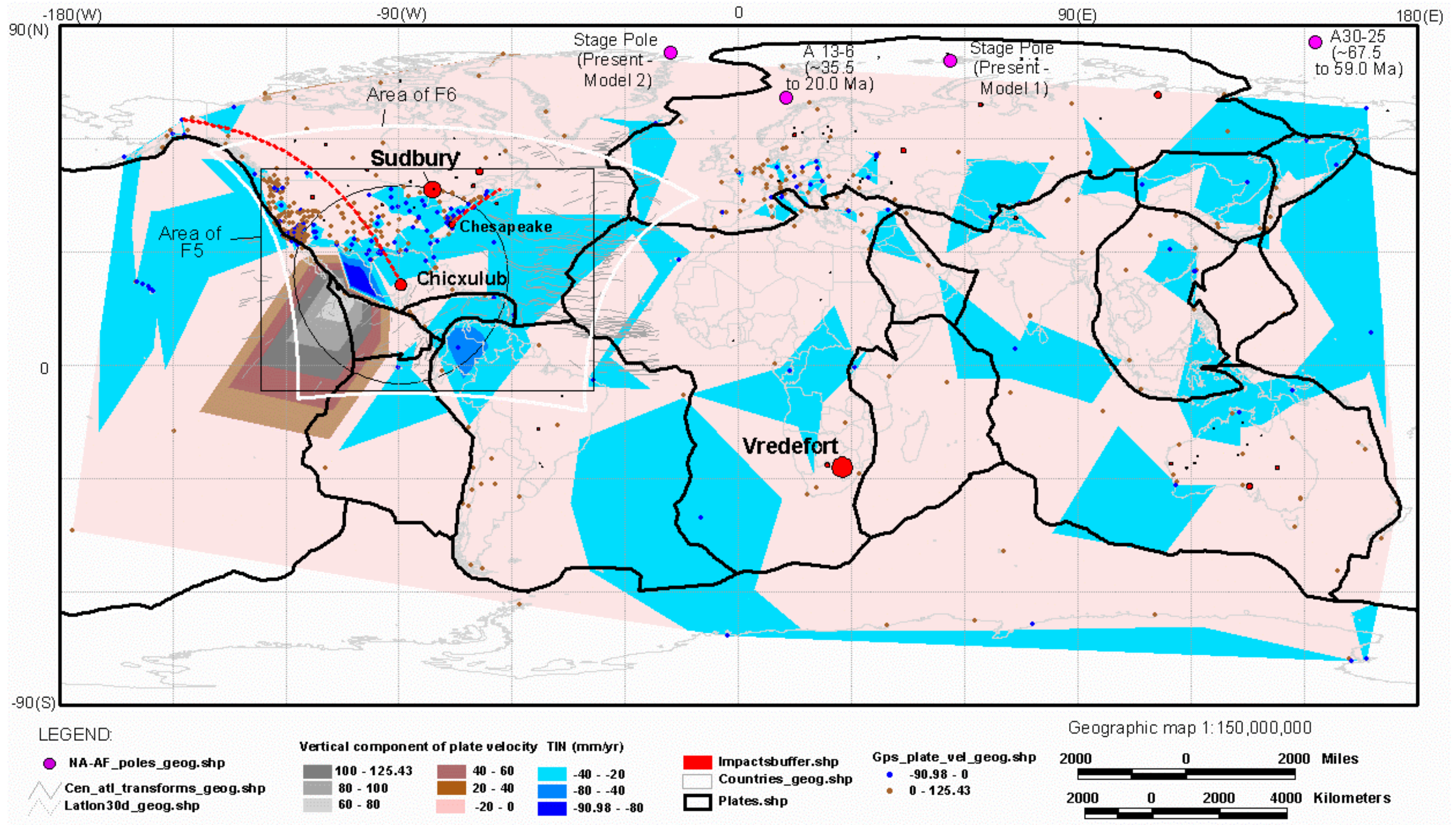
- The energy of the impact is estimated to be 6 million times more energetic than the 1980 Mount St. Helens volcanic eruption. The shock of the impact produced magnitude-10 earthquakes, greater than the magnitude of any we have ever measured in modern times.

- Geological and geophysical evidence collected over the last few years now suggests that Chicxulub could be the largest impact basin to form on Earth in the last billion years or so. (Eos, Vol. 76, December 26, 1995)

- The trajectory of impact has been estimated to be at about 20-30° with respect to the surface of the Earth and directed from the SE to NW based on atmospheric models of wildfire generation, fern spikes in the paleontology record, and the geometry of the impact crater

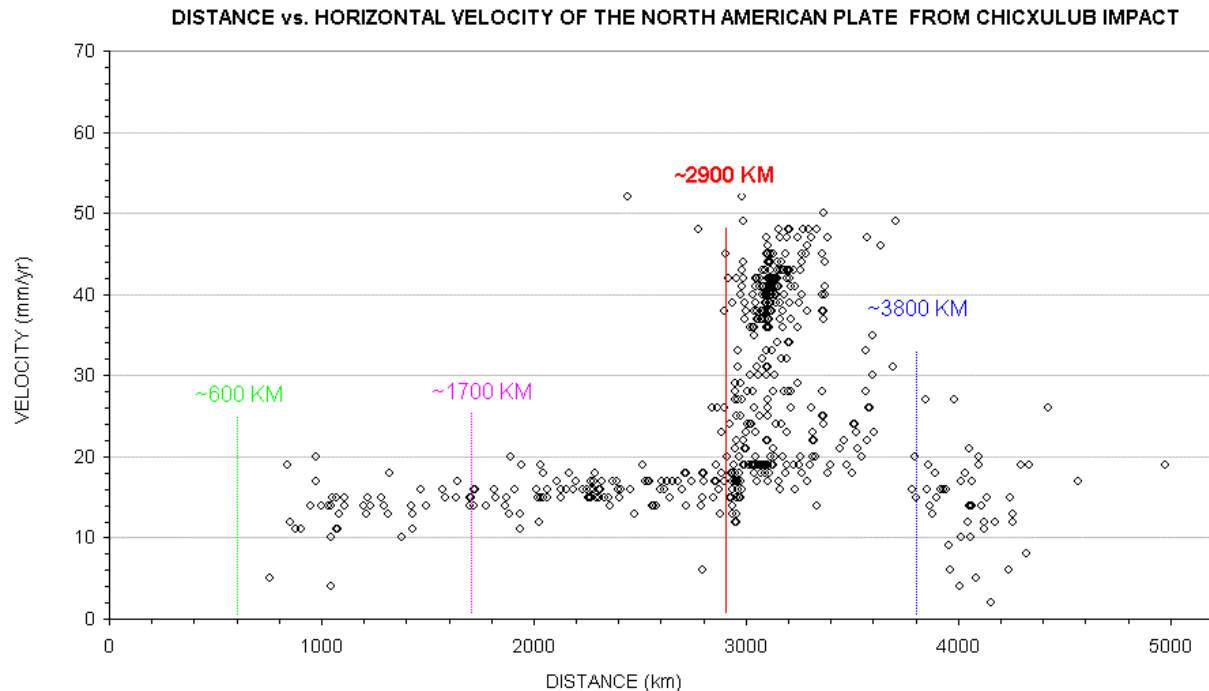


Note: The above material is adapted from: Discovering the Impact Site:
http://www.lpl.arizona.edu/SIC/impact_cratering/Chicxulub/Discovering_crater.html



Geographic map showing the location of NASA JPL GPS stations (778 worldwide from 1989 to 2005), equipotential map of vertical plate motions (using a triangulated integrated network (TIN) surface), 174 known terrestrial impact sites (buffered based on crater dimension), and select North America plate stage poles as summarized for DNAG (Klitgord and Shouten, 1986).

The horizontal component of plate motion for the North American plate versus distance from the Chicxulub impact shows a gradual, linear velocity increase up to about 2900 km distance, beyond which, velocities abruptly increase



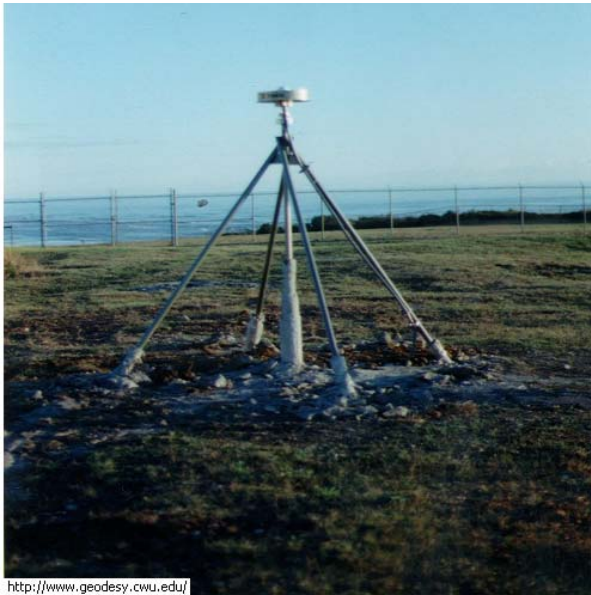
The 2900 km distance is the same as the depth from impact to the core-mantle boundary and therefore, today's plate kinematics may continue to signal a deep tectonic response to large, ancient impact events.

This led to a hypotheses that large scale, multi-ring impact structures stem from impact energy reflecting from major phase boundaries in the Earth's interior back to the surface to form circumferential arches and troughs in the crust.

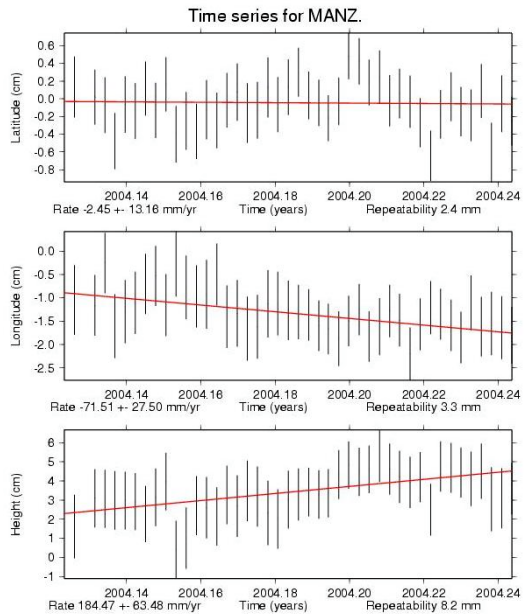
Moreover, because horizontal plate movement in the region appears circumferential to the impact point, large impacts such as Chicxulub probably play a much more significant role in plate tectonic theory than has been realized, and can apparently alter global plate dynamics

To investigate these hypotheses, GIS was employed to conduct various spatial analyses of past and neotectonic crustal activity including sea-floor spreading records in the west-central Atlantic region, historical seismicity, and current plate motions.

GPS_cartesian_plate_motion.xls																
	A	B	C	D	E	F	G	H	I	J	K	L	M	N	O	P
1	ID	STATION	TYPE	LAT	LON	HEIGHT	LATE	LONE	HE	TYPE	XVEL	YVEL	ZVEL	XERR	YERR	ZERR
2	1	BRMU	POS	34.594281880	-116.429378200	1337838.60	0.05	0.05	0.20	VEL	-20.22	-0.95	0.22	0.02	0.02	0.09
3	2	ISLK	POS	37.357958370	-115.158458200	1090011.00	0.11	0.13	0.41	VEL	-16.12	-10.56	-0.32	0.05	0.04	0.15
4	3	GLPT	POS	34.015004430	-119.363467700	22453.60	0.07	0.08	0.30	VEL	-46.92	11.41	-25.31	0.26	0.24	0.97
5	4	NRC2	POS	34.157442960	-118.830315800	246562.20	0.04	0.04	0.17	VEL	-40.08	18.25	1.51	0.04	0.02	0.09
6	5	LINJ	POS	36.319118840	-114.931788500	761058.70	0.13	0.21	0.51	VEL	-15.79	-9.68	1.26	0.09	0.06	0.23
7	6	WKPK	POS	36.050010750	-117.521943200	1791346.80	0.12	0.16	0.47	VEL	-19.17	-4.64	0.32	0.07	0.05	0.21
8	7	EGAN	POS	35.201251720	-118.910422100	76830.20	0.07	0.07	0.26	VEL	-25.22	4.91	2.06	0.08	0.07	0.29
9	8	COPO	POS	34.468300990	-117.153971100	888910.00	0.05	0.05	0.20	VEL	-26.21	2.45	-0.32	0.02	0.02	0.08
10	9	MDO1	POS	33.540072030	-116.629696000	1265713.40	0.05	0.05	0.19	VEL	-31.78	12.27	1.29	0.02	0.02	0.08
11	10	IRKJ	POS	34.126018010	-117.896485700	144765.50	0.08	0.08	0.34	VEL	-38.02	11.46	0.83	0.15	0.08	0.34
12	11	PBPP	POS	33.480450770	-119.029734300	14821.80	0.07	0.08	0.31	VEL	-41.36	21.25	2.33	0.23	0.21	0.86
13	12	PATT	POS	34.582197410	-119.981511500	204883.70	0.05	0.06	0.22	VEL	-39.40	20.10	3.40	0.15	0.09	0.35
14	13	GOSH	POS	34.264278540	-116.884240900	2051064.40	0.05	0.06	0.21	VEL	-23.88	5.89	0.90	0.02	0.02	0.09
15	14	MEM2	POS	34.920461340	-119.405847900	1332919.60	0.11	0.12	0.43	VEL	-33.18	12.88	4.85	0.50	0.29	1.17
16	15	TJRN	POS	34.000534140	-115.998190300	1373646.90	0.07	0.08	0.28	VEL	-16.76	-5.48	-1.03	0.20	0.18	0.73
17	16	CHZZ	POS	35.878387840	-118.074091700	2471209.00	0.06	0.06	0.23	VEL	-20.09	1.12	5.44	0.19	0.11	0.44



http://www.geodesy.cwu.edu/



http://sideshow.jpl.nasa.gov/mbh/series.html

Spatial analysis of GPS plate-motion data

obtained from the NASA JPL portal on the Internet World-Wide-Web for the geographic reference frame

3-axis velocity derivatives to map polar angles vector conversion using MS Excel:

Given horizontal velocity components with respect to the X- and Y-coordinate reference axes, the horizontal component of plate motion is a vector having magnitude (MAG in mm/yr) and azimuth bearing (AZM in degrees) determined as:

$$\text{MAG} = \text{SQRT} (\text{XVEL}^2 + \text{YVEL}^2) \text{ and } \text{AZM} = 360 + \text{THETA}$$

where SQRT is the square root function,

Then,

$\text{THETA} = \text{ATAN} (\text{X-COORD}, \text{Y-COORD})$, where ATAN is the arctangent of the specified x- and y- coordinates.

The arctangent is the angle from the x-axis to a line containing the origin (0, 0) and a point with X- and Y-coordinate values. The angle is given in radians between -p and p, excluding -p.

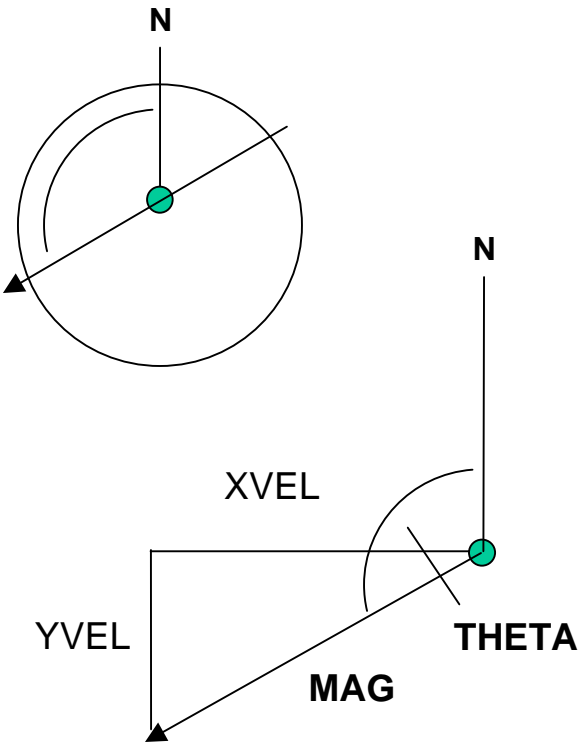
The Global Positioning System (GPS)

is a constellation of 30 satellites that is used for global navigation and precise geodetic position measurements (Assistant Secretary of Defense, 2001). Daily position estimates for each GPS receiver stations (ex. worksheet top left) are determined from satellite signals that are recorded by GPS receivers on the ground (ex. middle left photo). Data from various organizations and institutions that collect and analyze geodetic position information are catalogued and analyzed at the Jet Propulsion Laboratory, California Institute of Technology under contract with the National Aeronautics and Space Administration. GPS time-series data for each receiver location are analyzed (ex. below left) to determine the horizontal and vertical ground position of each location relative to the International Terrestrial Reference Frame (ITRF2000). The reference ellipsoid for latitude, longitude, and height is WGS84 (ref). Latitude and longitude are given in degrees. Height, geographic positions, and positional errors are given in mm. Velocities and their errors are given in mm/yr.

Q3

=DEGREES(ATAN2(L3, K3))

GPS_cartesian_plate_motion.xls																	
	C	D	E	F	G	H	I	J	K	L	M	N	O	P	Q	R	S
1	TYPE	LAT	LON	HEIGHT	LATE	LONE	HE	TYPE	XVEL	YVEL	ZVEL	XERR	YERR	ZERR	THETA	AZM	MAG
2	POS	34.594281880	-116.429378200	1337838.60	0.05	0.05	0.20	VEL	-20.22	-0.95	0.22	0.02	0.02	0.09	-92.69	267	20
3	POS	37.357958370	-115.158458200	1090011.00	0.11	0.13	0.41	VEL	-16.12	-10.56	-0.32	0.05	0.04	0.15	-123.228	237	19
4	POS	34.015004430	-119.363467700	22453.60	0.07	0.08	0.30	VEL	-46.92	11.41	-25.31	0.26	0.24	0.97	-76.3321	284	48
5	POS	34.157442960	-118.830315800	246562.20	0.04	0.04	0.17	VEL	-40.08	18.25	1.51	0.04	0.02	0.09	-65.5184	294	44
6	POS	36.319118840	-114.931788500	761058.70	0.13	0.21	0.51	VEL	-15.79	-9.68	1.26	0.09	0.06	0.23	-121.51	238	19
7	POS	36.050010750	-117.521943200	1791346.80	0.12	0.16	0.47	VEL	-19.17	-4.64	0.32	0.07	0.05	0.21	-103.606	256	20
8	POS	35.201251720	-118.910422100	76830.20	0.07	0.07	0.26	VEL	-25.22	4.91	2.06	0.08	0.07	0.29	-78.9831	281	26
9	POS	34.468300990	-117.153971100	888910.00	0.05	0.05	0.20	VEL	-26.21	2.45	-0.32	0.02	0.02	0.08	-84.6598	275	26
10	POS	33.540072030	-116.629696000	1265713.40	0.05	0.05	0.19	VEL	-31.78	12.27	1.29	0.02	0.02	0.08	-68.8888	291	34
11	POS	34.126018010	-117.896485700	144765.50	0.08	0.08	0.34	VEL	-38.02	11.46	0.83	0.15	0.08	0.34	-73.2261	287	40
12	POS	33.480450770	-119.029734300	14821.80	0.07	0.08	0.31	VEL	-41.36	21.25	2.33	0.23	0.21	0.86	-62.8067	297	46
13	POS	34.582197410	-119.981511500	204883.70	0.05	0.06	0.22	VEL	-39.40	20.10	3.40	0.15	0.09	0.35	-62.9715	297	44
14	POS	34.264278540	-116.884240900	2051064.40	0.05	0.06	0.21	VEL	-23.88	5.89	0.90	0.02	0.02	0.09	-76.1446	284	25



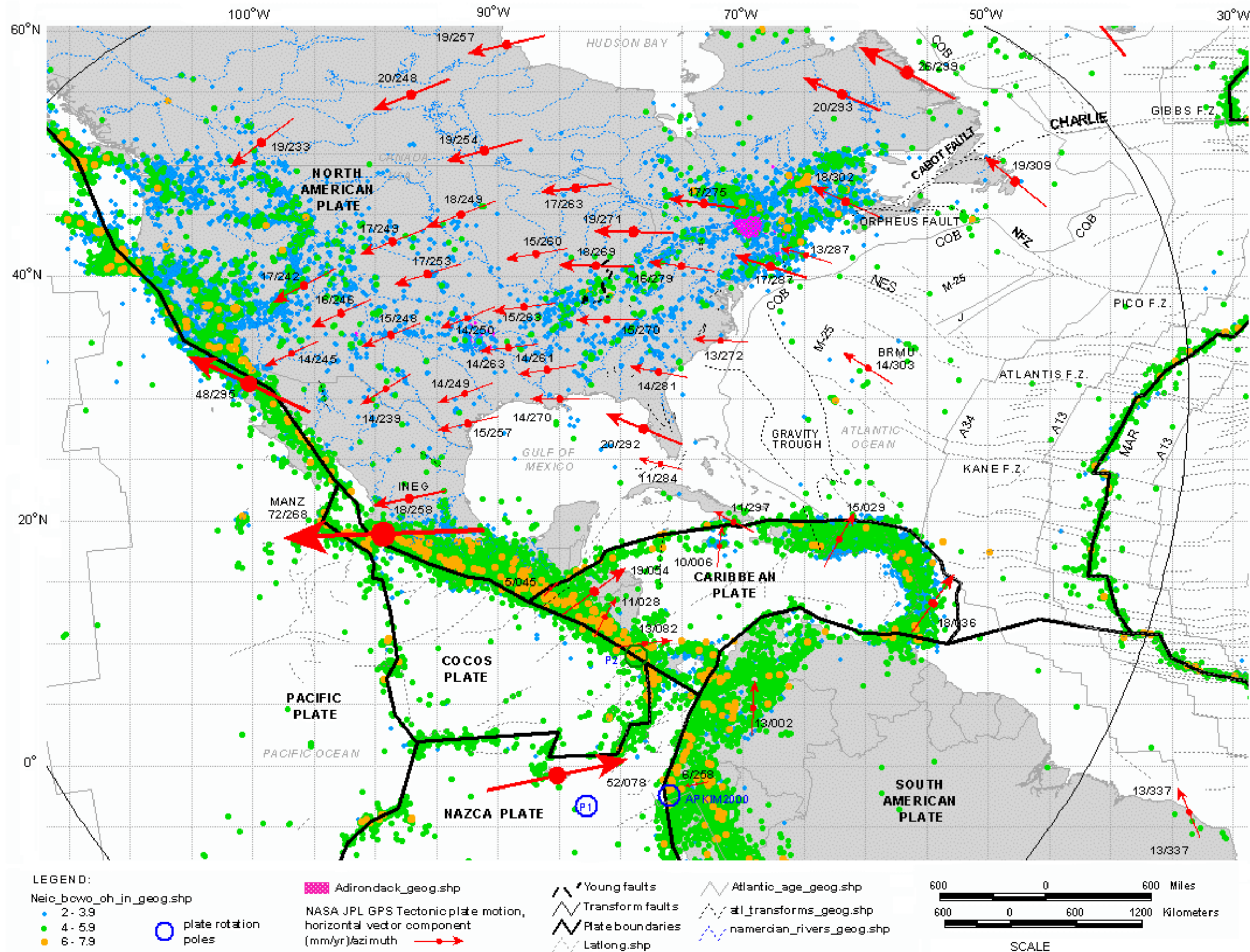
ATAN(THETA)

XVEL + THETA (0 to 180)

XVEL - THETA (0 to -180)

THETA = -123

AZM = 267 (360 + (-123))



The North American plate (NAP) and other plates in the Central American region display circumferential motion about the location of the ~65 Ma Chicxulub impact.

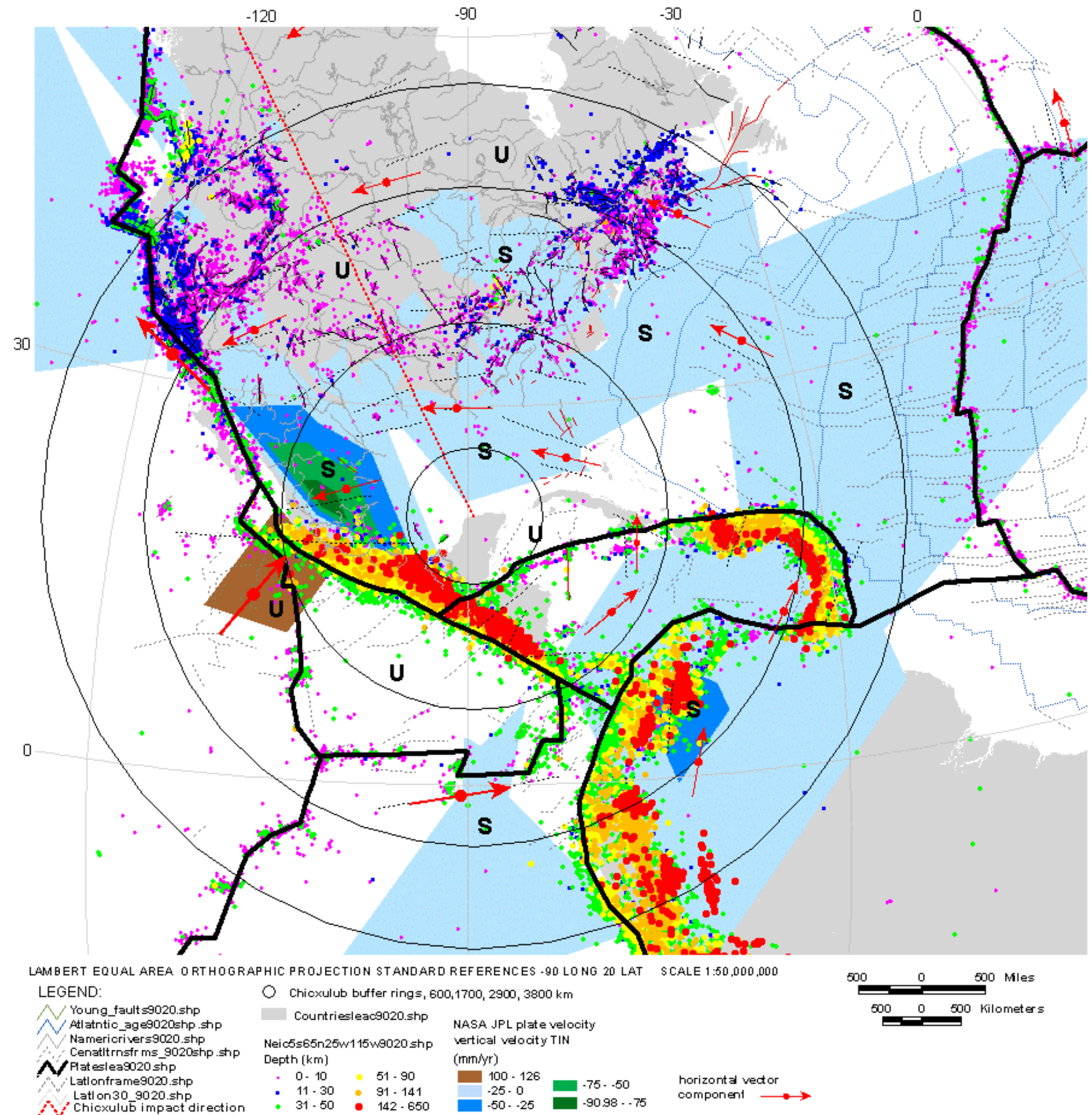
Map shows major plate boundaries, sea-floor shear-zones lineaments and select magnetic isochrons in the west-central Atlantic Ocean, NASA GPS horizontal plate-motion vectors, USGS NEIC and other historical seismicity records for events \geq magnitude 2.0 (see F5) for the North and Central America regions, and North American plate actual rotation poles from the NUVEL-1A and APKIM2000 models

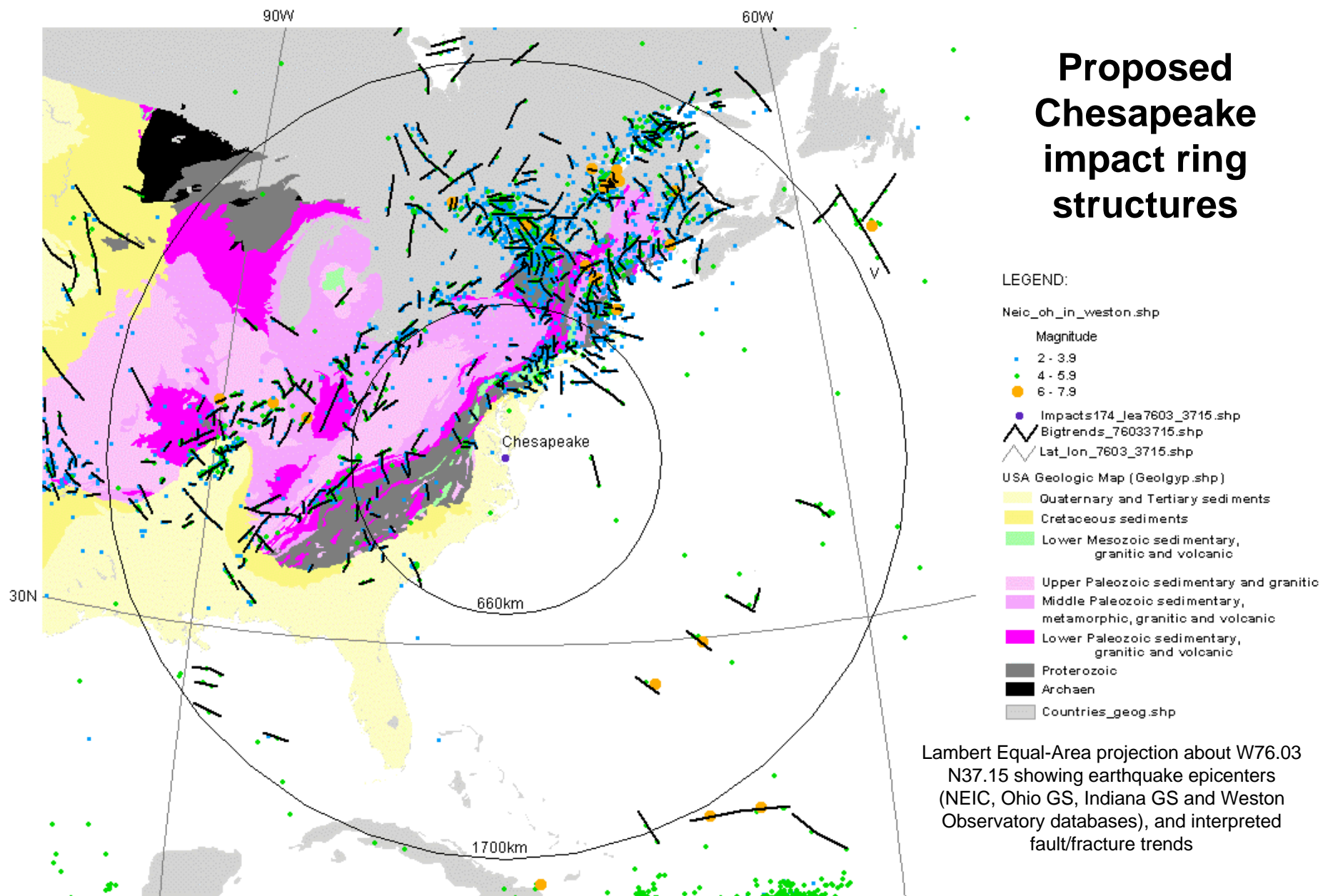
An orthographic projection about the impact point was used to explore spatial symmetry between current earthquake seismicity and the multi-ring basin and arch hypothesis.

Current areas of mid-continental uplift and subsidence display circumferential symmetry with respect to the rings as do mid-continental and eastern seismogenic zones (F7), crustal geology (F8), Bouger gravity anomalies in the Gulf of Mexico and western Atlantic regions (F9) and continental physiography (F10).

The Adirondack and Laramide epeirogenic uplifts reportedly began in the Tertiary and are centered on the 2900 km ring (F7)

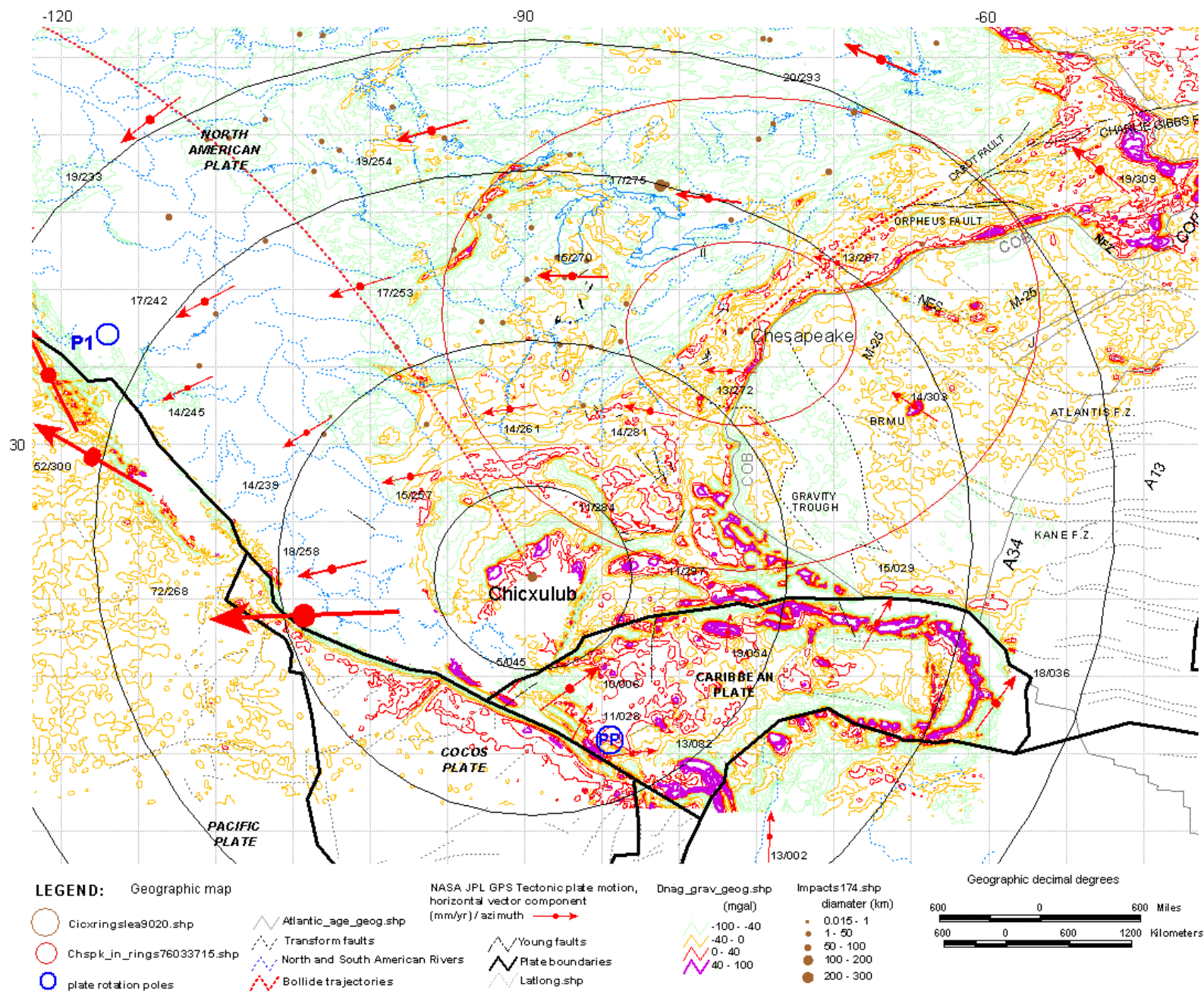
Map shows multi-ring impact structures proposed to stem from the Chicxulub impact event, tectonic plate boundaries, historical earthquake seismicity filtered by depth, select recent and current fault trends, sea-floor spreading shear-zone lineaments, select magnetic isochrons, NASA GPS Plate-motion vectors and elements of the vertical component of plate motion displayed as a TIN for the North and Central America regions.





F7a

Herman, G. C., 2006, [Neotectonic setting of the North American Plate in relation to the Chicxulub impact](#): Geological Society America Abstracts with Programs, Vol. 38, No. 7, p. 415



DNAG Bouger gravity showing proposed multi-ring structures

F7b

Herman, G. C., 2006, [Neotectonic setting of the North American Plate in relation to the Chicxulub impact](#): Geological Society America Abstracts with Programs, Vol. 38, No. 7, p. 415

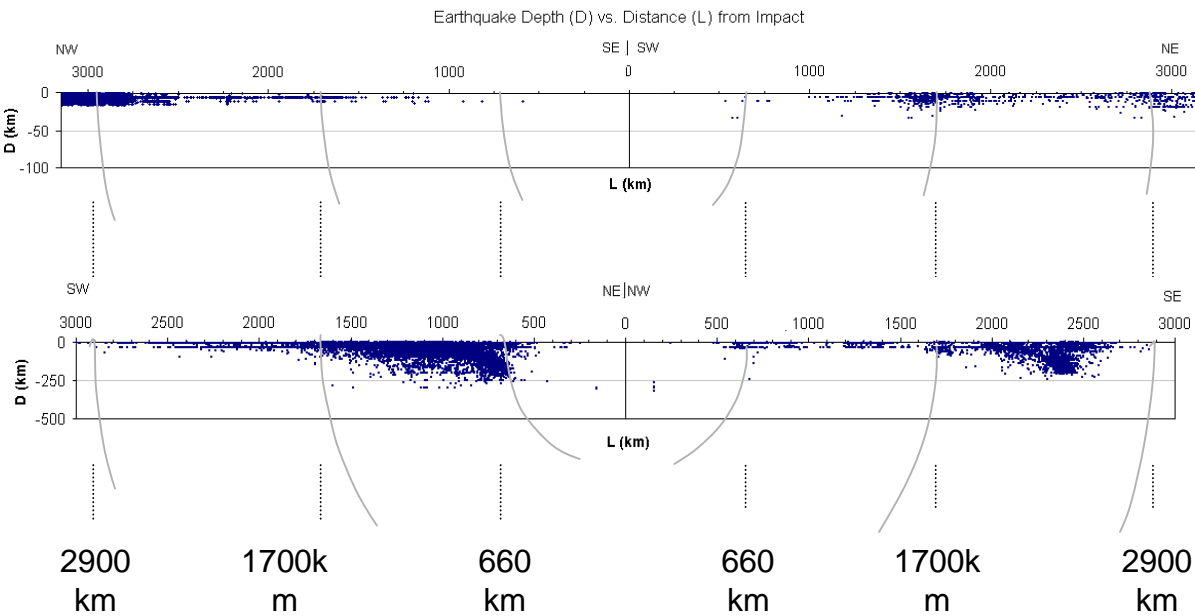
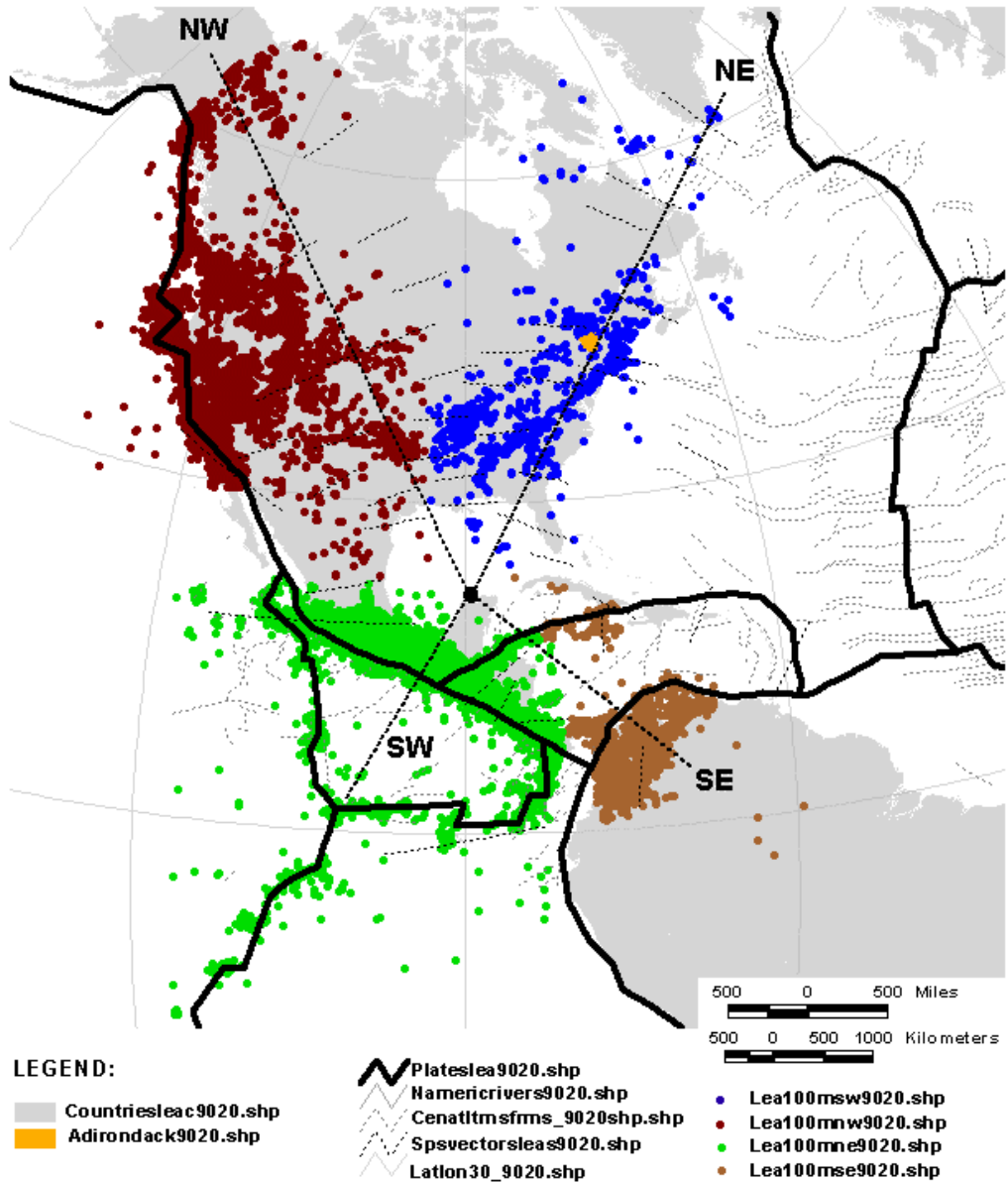
Spatial analysis of seismogenic zones in the mid-continental and eastern parts of the NAP with respect to the multi-ring impact structure hypothesis

Records of historical earthquake seismicity in the region were obtained from WWW portals maintained by the U.S. Geological Survey (USGS, the Boston College Weston Observatory, the New Jersey Geological Survey, the Ohio Geological Survey, and the Indiana Geological Surveys. The records of historical earthquakes include both instrumental and noninstrumental earthquake locations and magnitudes. Noninstrumental events stem from a variety of historical accounts including newspaper articles, scientific publications, government reports and records. Non-instrumental epicenter locations are significantly less accurate in comparison to instrumental epicenter locations. Catalog information for instrumental events vary from somewhat to highly accurate depending on the instruments and instrument spread used to identify the epicenters.

A computer-based search for earthquake events from the USGS National Earthquake Information Center (NEIC) on January 20, 2005 returned a list of 266,862 earthquake events for the period of 1973 to 2001 in the region between 90N to 90S latitudes and 30E to 150W longitudes. The Weston Observatory data include three different catalogs for events recorded before 1990, from 1990 to 1999 and from 2000 to 2005. Those data having geographic coordinates includes 3602 events occurring between latitudes 39N to 60N and longitudes 46W to 83W. The New Jersey earthquake catalog includes 320 events through 1990 between latitudes 38N to 42N and longitudes 72W to 76W. The Ohio catalog includes 179 events recorded from 1776 to 2004 between latitudes 38N to 42N and longitudes 80W to 85W. The Indiana catalog includes 59 events recorded from 1827 to 2002 between latitudes 38N to 42N and 72W to 77W. Many events recorded in the Weston Observatory and State catalogs are included in the USGS catalog. Earthquake events greater than or equal to magnitude 2 having geographic coordinates in the NEIC, Weston, Ohio and Indiana catalogs were combined into a single database list and parsed to eliminate duplicate records. A GIS point theme was produced from the combined results using the Environmental Systems Research Institute, Inc. (ESRI) shapefile format. The resulting coverage has 28,139 events. Of this total 26,625 include depth values and 27,852 are greater than or equal to magnitude 2.0.

Seismic zones were mapped from the NEIC records using the ArcView GRID program. Densities of earthquake epicenters (events/sq. km) were calculated using a 1-degree cell size and a search radius of 50 km, then displayed using a range of density values as shown in figures F9, F10, and F11.

A spatial analysis of historical earthquake seismicity versus distance and depth is shown to the right relative to the Chicxulub impact point. Depths of historical earthquakes versus distance from impact were plotted along four quadrants to investigate spatial relationship between upper mantle and crustal seismicity with respect to the proposed multi-ring architecture of the Chicxulub impact



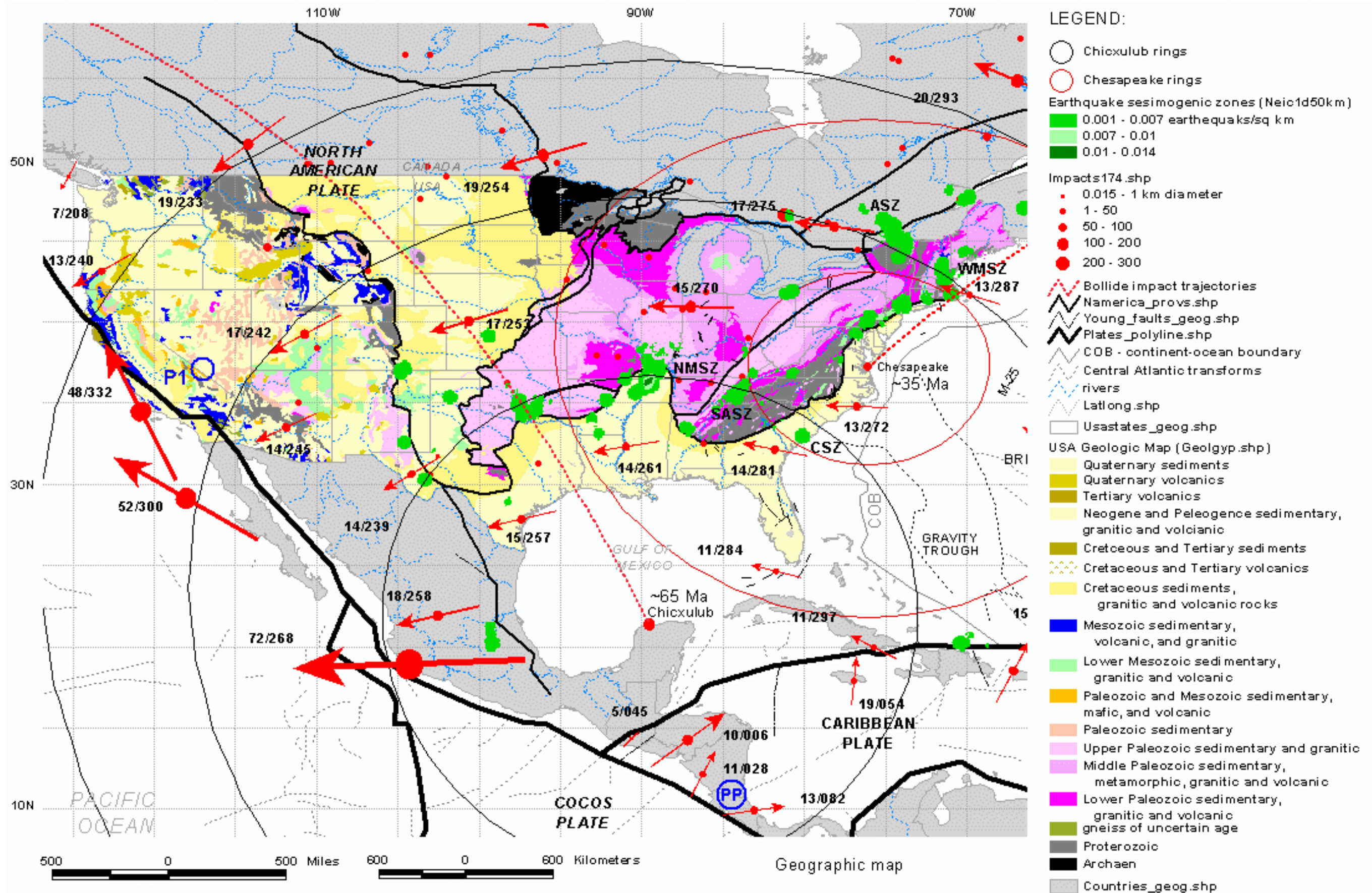
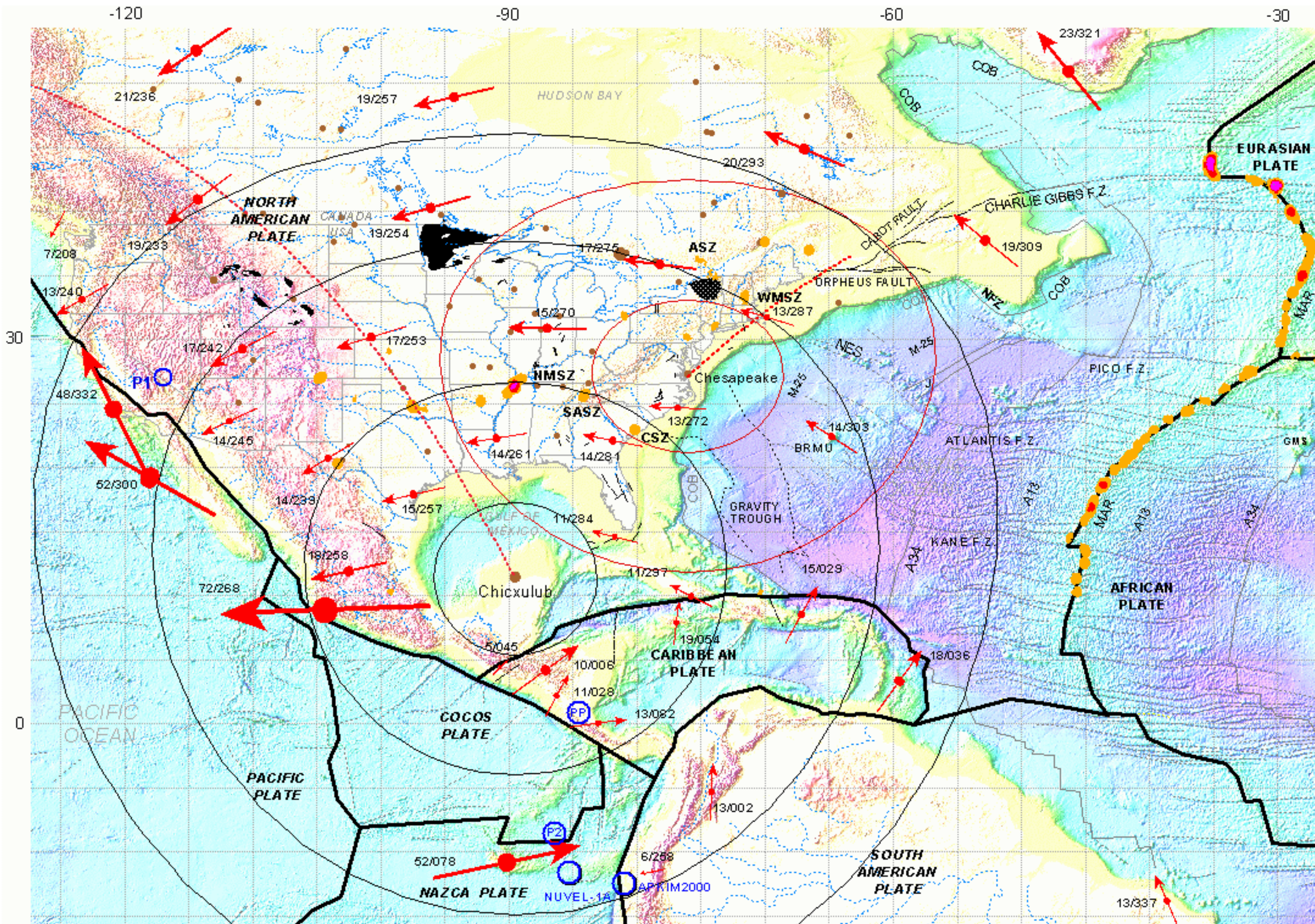


Plate boundaries, NASA GPS horizontal plate-motion vectors, seismogenic zones, and proposed multi-ring structures stemming from the Chicxulub and Chesapeake impacts with respect to physiographic regions of North America and a generalized geological map of the United States



Chicxulub and Chesapeake impact ring structures (proposed), crustal physiography showing-floor spreading lineaments, NASA GPS horizontal plate-motion vectors, historical earthquake seismic zones (north of 20° latitude and east of 105° longitude) based on USGS NEIC database, and known impact locations, North and Central America regions.

Spatial analysis of GPS plate-motion data to determine an actual rotation pole for the NAP

Actual plate-rotation poles were calculated for the North American tectonic plate using a custom ArcView GIS Avenue script.

The script calculates the normal ray path to the horizontal direction of plate motion at each GPS site, and then intersects each ray path with all other ray paths determined for a selected set of GPS stations.

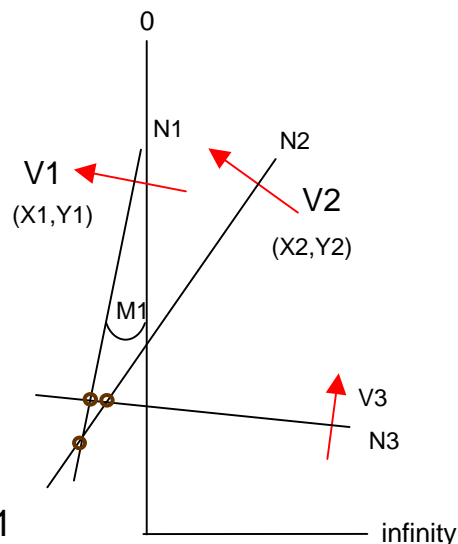
Plate-rotation poles are assumed to correspond to the densest clusters of resulting intersection points, determined using the ArcView GRID program, a cell-based spatial analysis program. This approach assumed that GPS plate-motion data reflect plate rotation about a pole.

Using the slope-intercept equation: $Y = MX + B$ (or $B = Y - MX$)
Calculate B_1 for a vector-normal line (N_1) with known slope (M_1)
at the location of the GPS station (X_1 and Y_1)

$\text{RadBearing} = \text{Bearing} * \text{Radian}$
 $M_1 = \text{RadBearing.Tan} * -1$
 $B_1 = Y_1 - (M_1 * X_1)$
where M_1 is the SLOPENORMAL

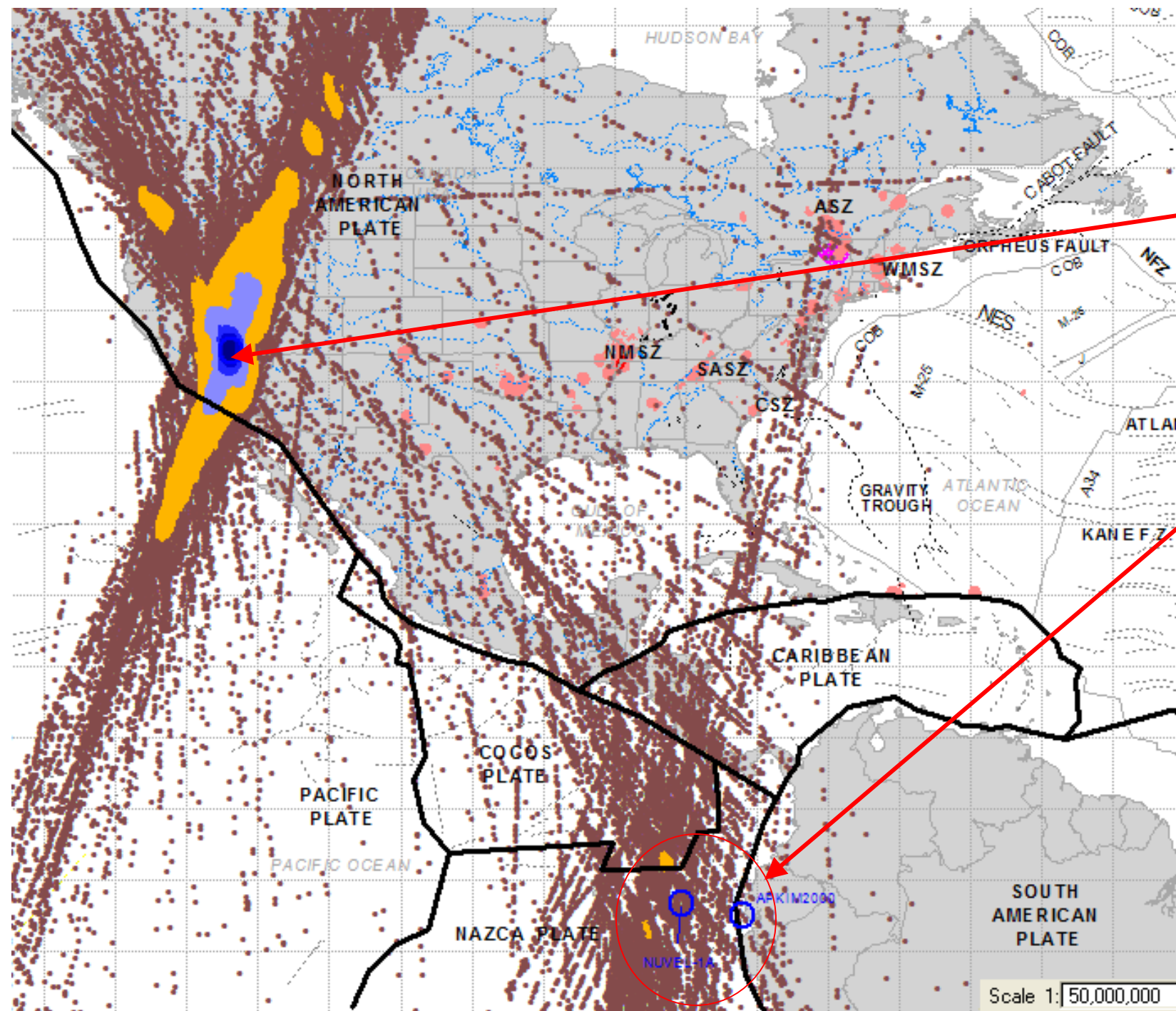
and similarly for each other vector:

$B_n = Y_n - (M_n * X_n)$
 $B_{\text{minus}} = B_n - B_1$
 $X_{\text{intercept}} = B_{\text{minus}} / X_{\text{minus}}$
 $Y_{\text{intercept}} = (\text{SlopeNormal} * X_{\text{intercept}}) + B_1$



Loop through the calculation of $B_n...$ and $M_n..$ for the remainder of the stations, calculating point of intersections for N_1 and all other vector-normal rays.

Run successive loops for N_2 to $N_n...$



NAP Plate-rotation analysis with all GPS stations selected on the North American Plate

Primary cluster of intersection points is located near the SW margin of the basin and range province where plate motion begins changing from NAP to Pacific trends

Actual plate-rotation pole(s) map west of Ecuador near rotation poles determined from NUVEL-1A and APKIM2000 plate-rotation models for the NAP

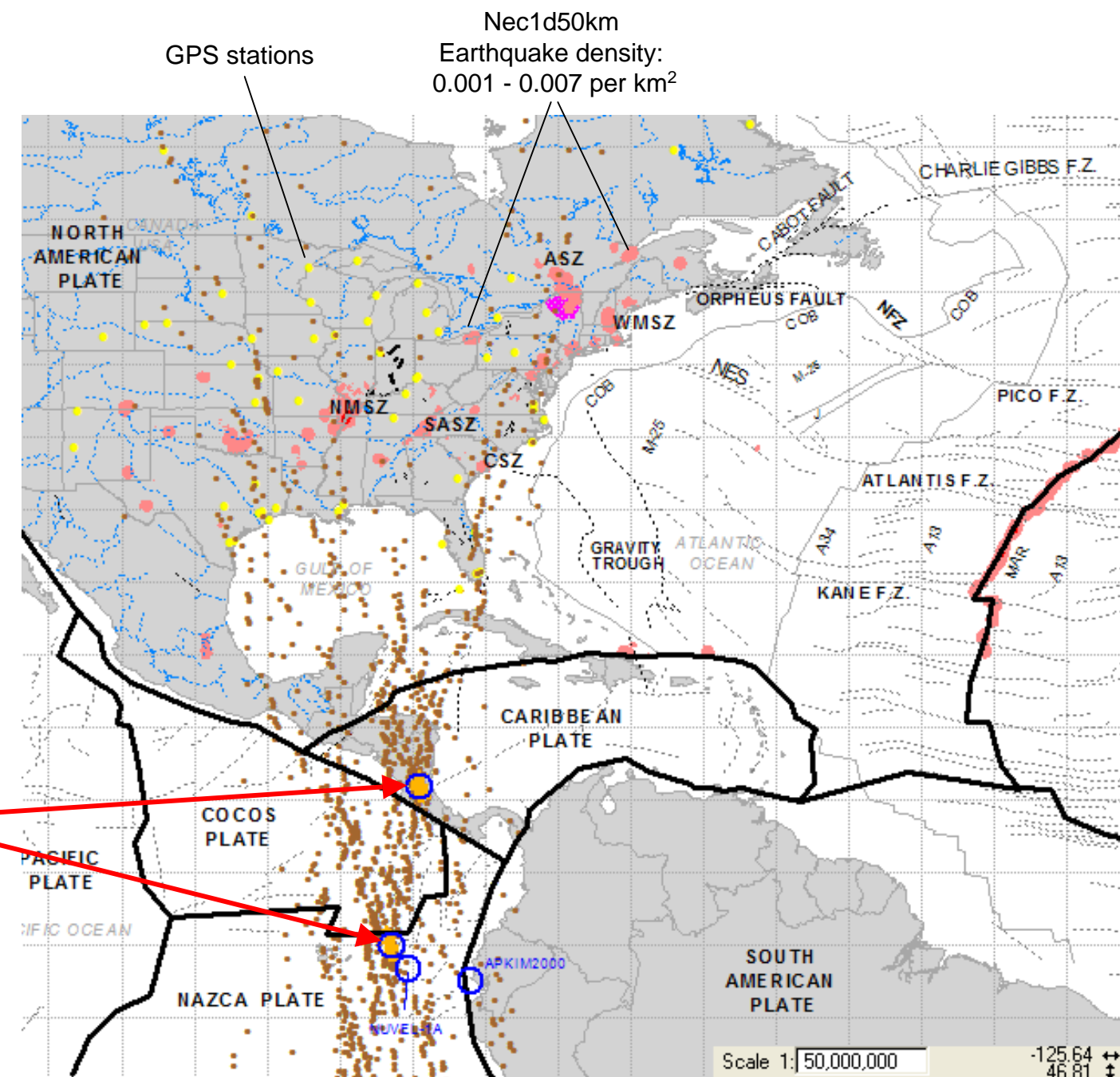
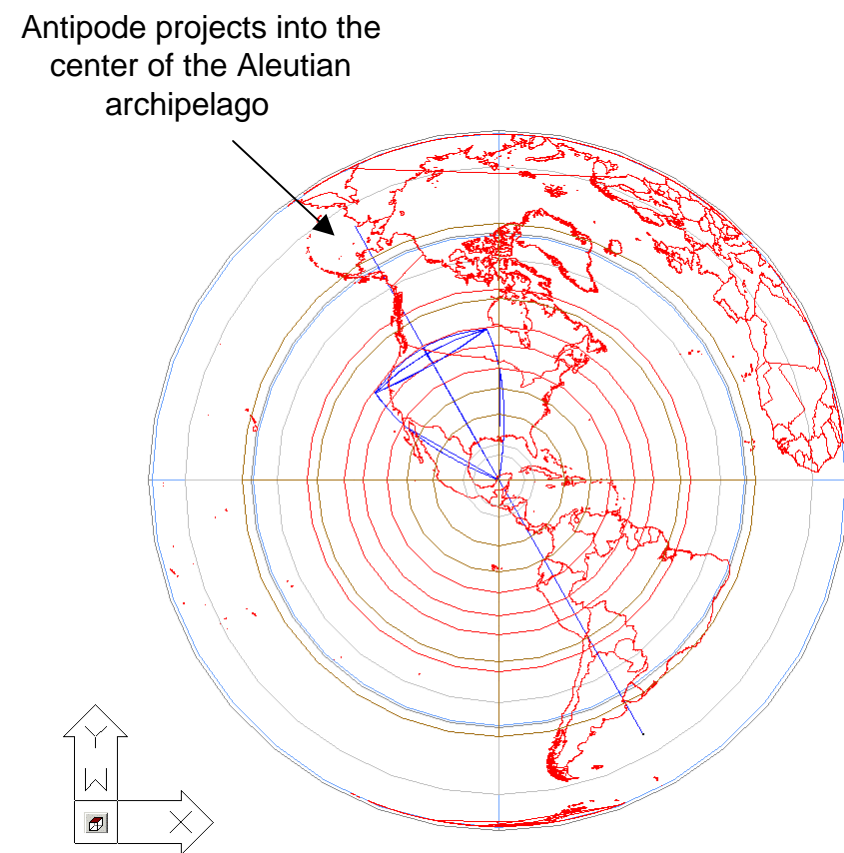
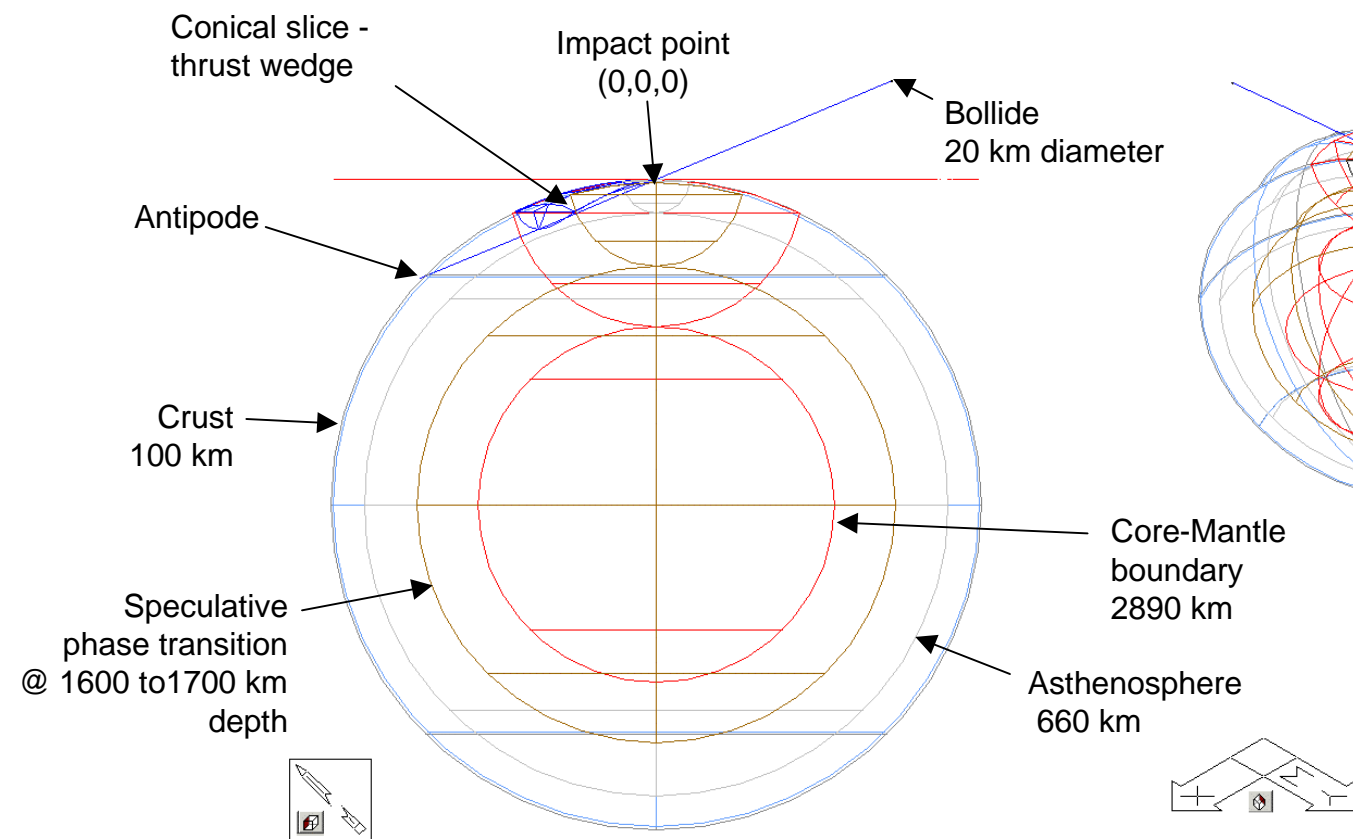


Plate-rotation analysis with subsets of GPS stations selected on the North American Plate

Subsequent analyses that exclude GPS data in the western orogenic belts and stations near active seismogenic zones in mid-continental and eastern regions result in a , 'stable craton' rotation-pole solutions west of Equador and near Panama, suggesting the occurrence of sub-plate rotations within the NAP



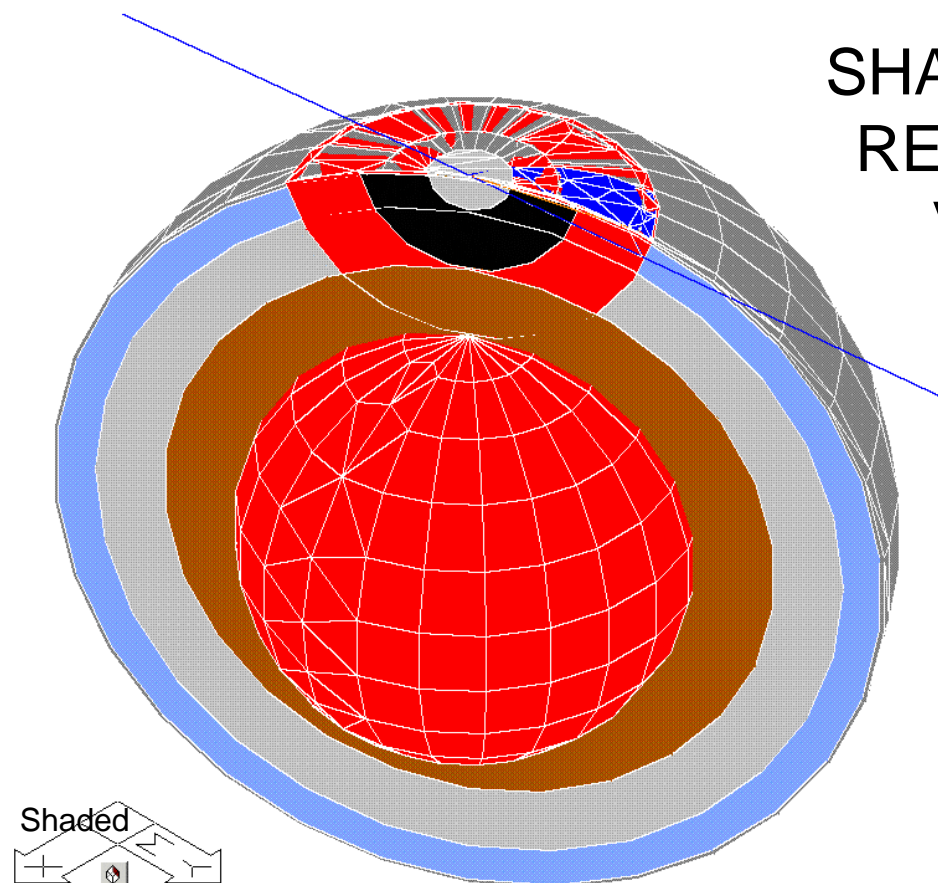
MAP VIEW



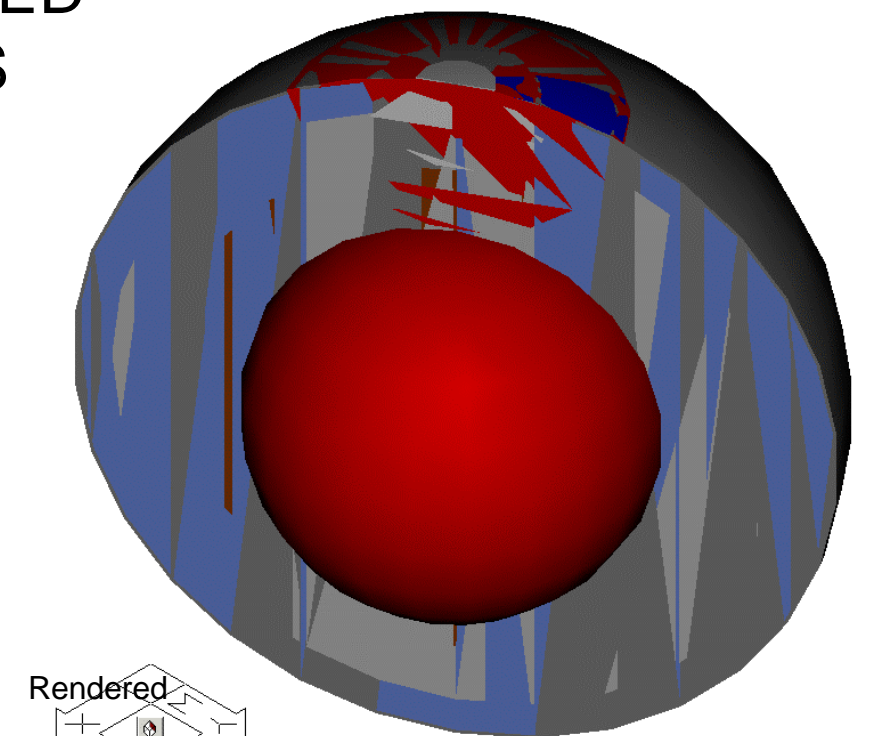
PROFILE VIEW

NE SYMMETRIC VIEW

AutoCAD solid object earth model used to explore 3-dimensional geometry of spherical percussion shells reflective of Earth's compositional layers

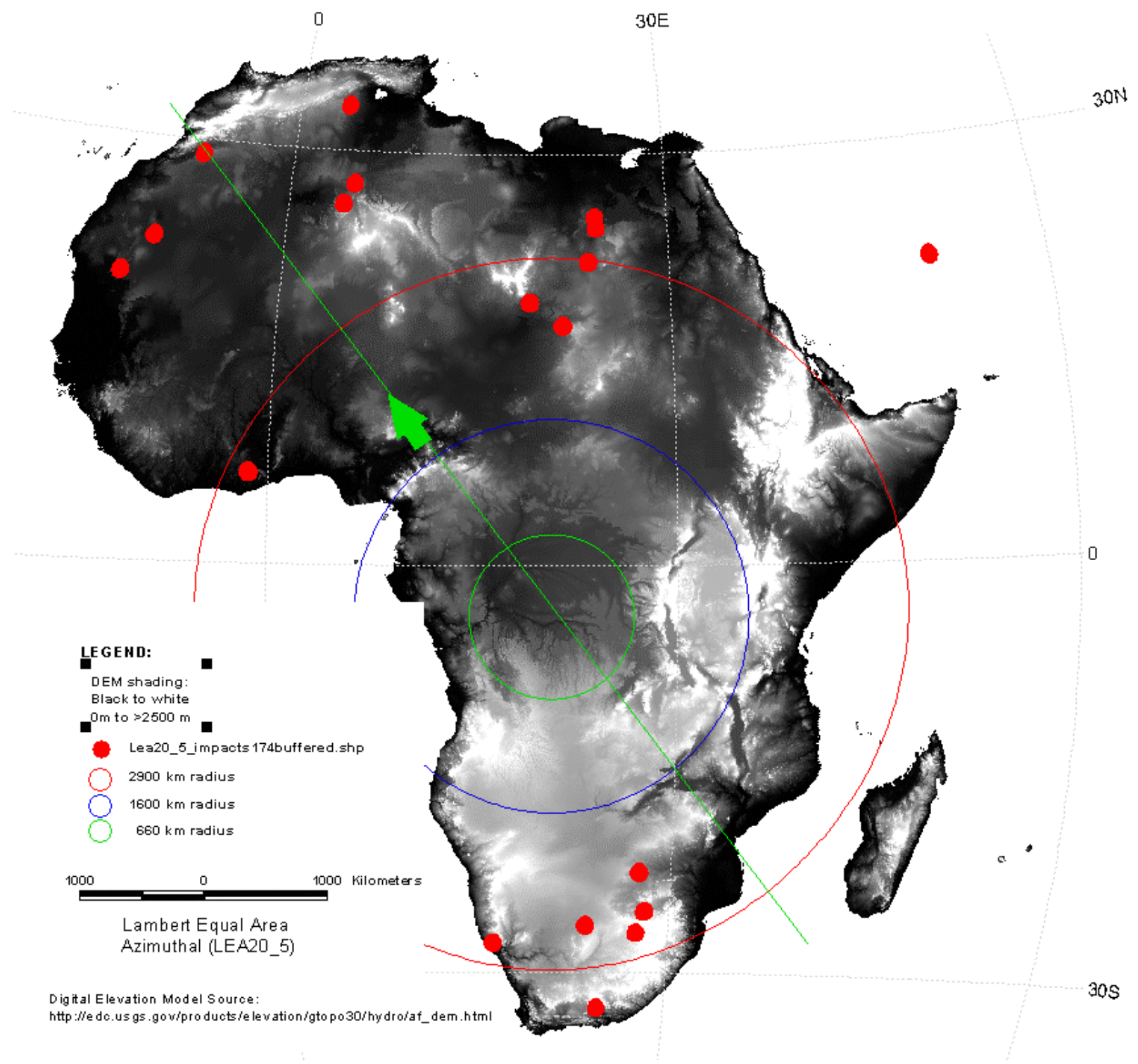
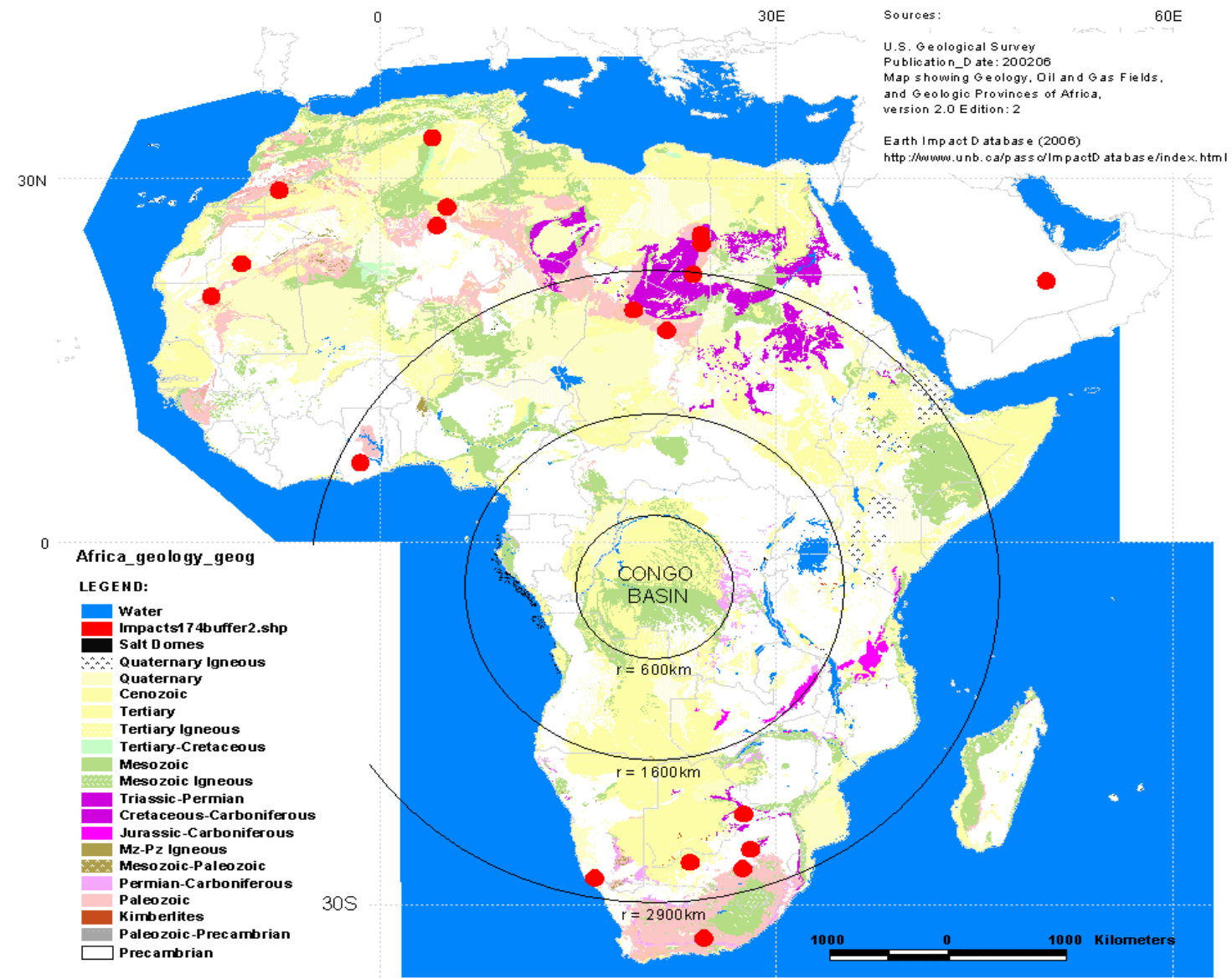


SHADED AND RENDERED VIEWS



SEARCH FOR CORROBORATIVE PROOF

The Congo basin has not been investigated with respect to being an impact structure. The basin is centered on the combined African, Somali, and Arabia plates, is surrounded by symmetric, leaky transform faults, and has associated strata reflective of a Permian-Triassic age impact event. Could this basin be a result of fragmented bolide event contributing to the breakup of Pangea?



Digital elevation model (above) and generalized geological map of Africa (right) with the Congo basin at the center of a multi-ringed impact basin having similar dimensions as hypothesized for the Chicxulub event.